

Supporting Information

Polyamine Functionalized Imidazolyl Poly(ionic liquid)s for the Efficient Conversion of CO₂ into Cyclic Carbonates

Yizhen Zou, Yuansheng Ge, Qiang Zhang, Wei Liu, Xiaoguang Li, Guo Cheng and Hanzhong Ke
*

Faculty of Materials Science and Chemistry, China University of Geosciences (Wuhan), 388 Lumo Road, Wuhan 430074, China.

Table of Contents

General information.....	1
XRD and TGA of N ₄ -PIL-2.....	2
The ¹ H NMR spectrums.....	3
Comparisons of the catalytic activity of N ₄ -PIL-2.	8
Cartesian Coordinates (Å) of the Optimized Structures.	10
References.....	14

General information

All the epoxide substrates used were of analytical grade, and sourced from Energy Chemical of Anhui Zesheng Technology Co., Ltd. (Shanghai, China). Divinylbenzene (DVB) and solvents were purchased from Sinopharm Chemical Reagent Co., Ltd. DVB was treated to remove the polymerization inhibitor before use. All the solvents were used as received without further purification.

Micromeritics ASAP 2460 system was operated to measure nitrogen adsorption and desorption isotherms at the liquid-nitrogen temperature of 77 K, the samples were degassed in vacuum at 120 °C for 10 h before analysis , their surface areas and pore size distribution, pore volumes of samples were calculated by the Brunauer–Emmett–Teller (BET) equation and non-local density functional theory (NLDFT) model. Fourier transform infrared spectroscopy (FT-IR) spectrum were obtained from a Nicolet 6700 spectrophotometer ranging from 4000 to 400 cm⁻¹ by using KBr pellets. ¹H NMR spectra were identified on a Bruker Avance III HD 400 MHz spectrometer with the solvent D₂O and internal reference tetramethylsilane (TMS) at room temperature. Solid-state ¹³C CP/MAS NMR was registered in a Brucker 400M with 12 kHz spinning rate. The crystal phase of synthesized

samples was identified by X-ray diffraction (XRD, Bruker AXS D8-Focus, Germany) with Cu K α radiation over the range of 2 θ from 5° to 70°. A Netzsch STA 449 F3 thermogravimeter was employed to provide Thermogravimetric analysis (TGA) from 30 to 700 °C at the heating rate of 10 K min⁻¹ under dry air. The content of C, H, N elements and their distribution were obtained from a CHN elemental mode of Vario EL cube and elemental mapping in scanning electron microscope (SEM), respectively. SEM was characterized the morphologies and structures of the samples by a SU8010 model Hitachi microscope. The DFT calculations was performed on BIOVIA Materials Studio 2017, the geometry optimizations were conducted by using the GGA-PW91 functional together with the Effective Core Potentials core treatment and DNP basis set.

XRD and TGA of N₄-PIL-2

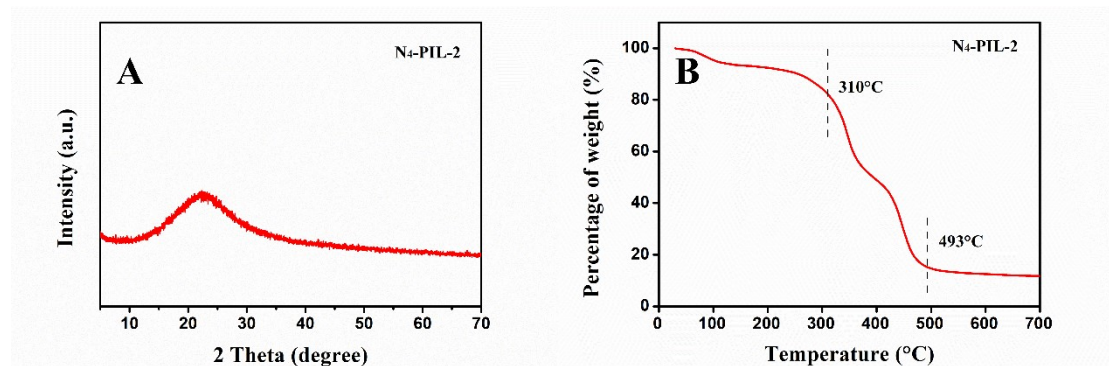
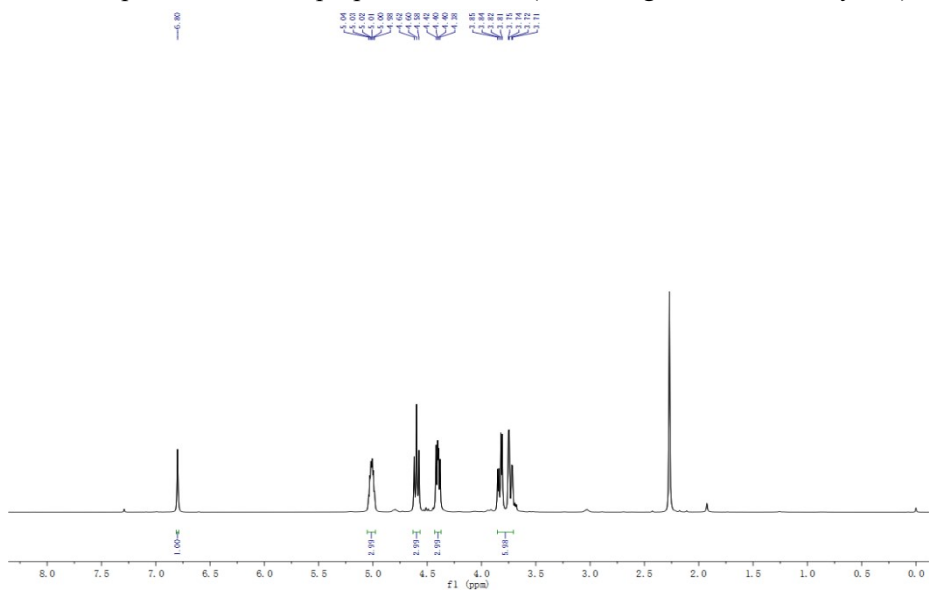


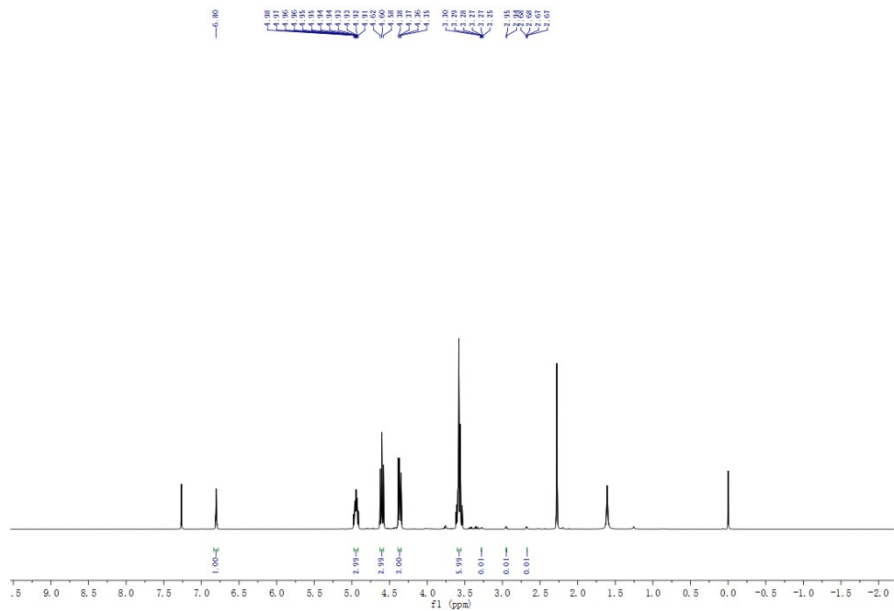
Fig. S1. (A) XRD patterns of the N₄-PIL-2; (B) TGA curves of N₄-PIL-2.

The ^1H NMR spectra

^1H NMR of crude product of chloropropene carbonate (containing 10 mol % mesitylene)



^1H NMR of crude product of cyclic carbonate from 2-(bromomethyl)oxirane (containing 10 mol % mesitylene)



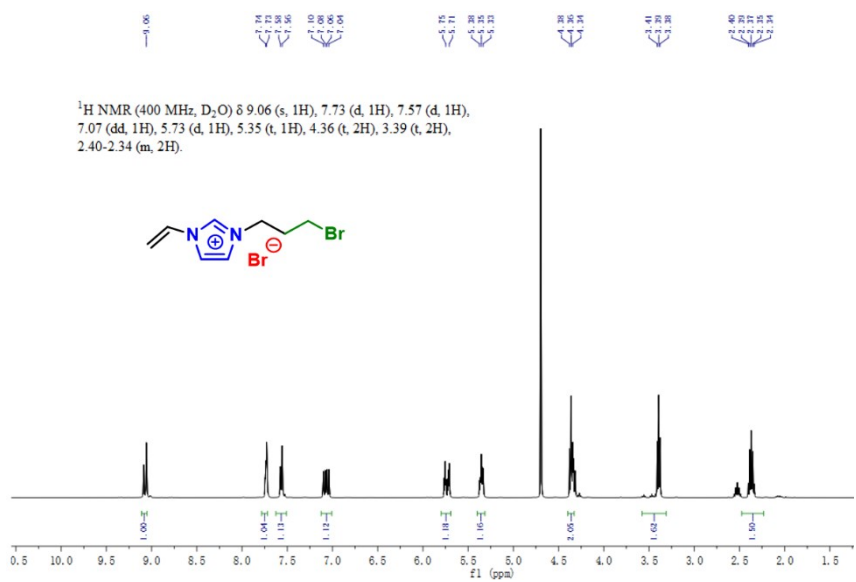


Fig. S2. ¹H NMR spectrum of VIMBr in D_2O (Scheme 1).

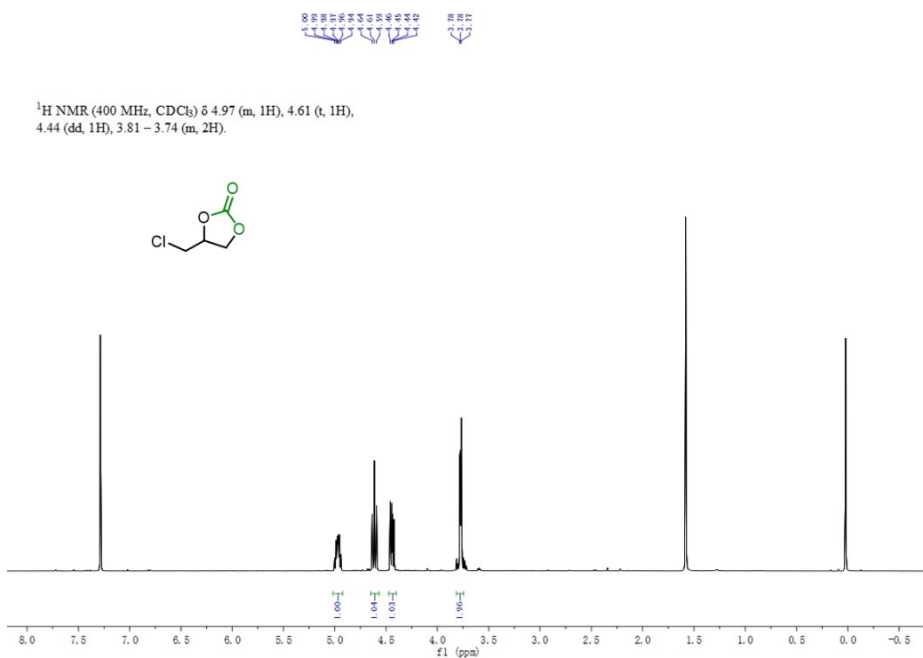


Fig. S3. Crude ¹H NMR spectrum of cyclic carbonate from epichlorohydrin in CDCl_3 (Table 4, entry 1).



^1H NMR (400 MHz, CDCl_3) δ 4.97 (m, 1H), 4.61 (t, 1H), 4.44 (dd, 1H), 3.81 – 3.74 (m, 2H).

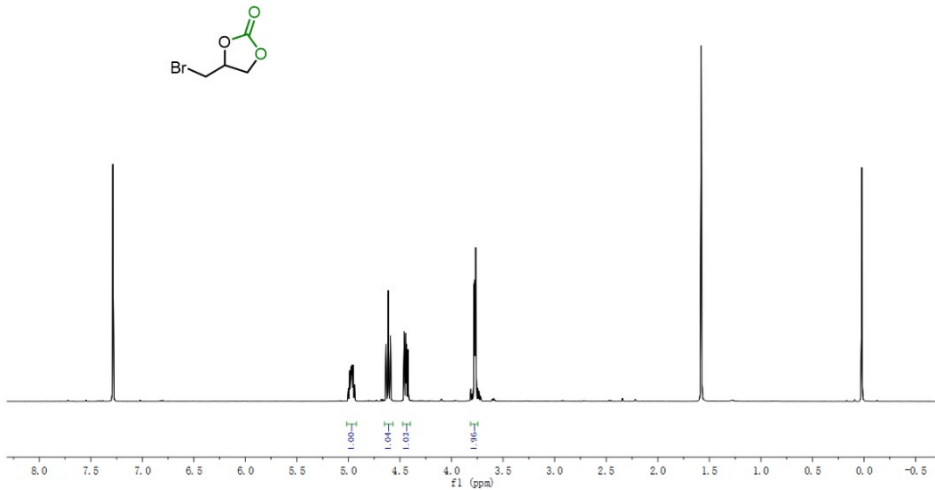


Fig. S4. Crude ^1H NMR spectrum of cyclic carbonate from 2-(bromomethyl)oxirane in CDCl_3 (Table 4, entry 3).



^1H NMR (400 MHz, CDCl_3) δ 4.87 (ddd, 1H), 4.59 – 4.50 (m, 1H), 4.03 (dd, 1H), 1.50 (d, 3H).

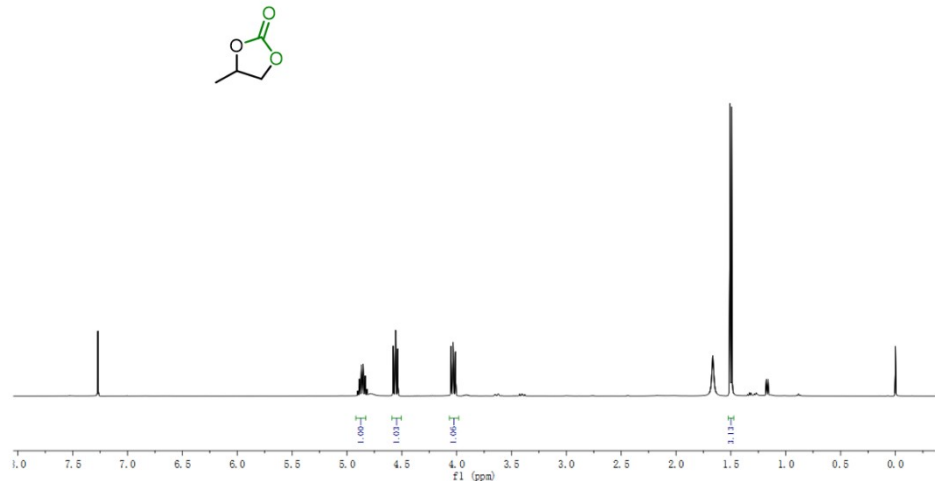


Fig. S5. Crude ^1H NMR spectrum of cyclic carbonate from propylene oxide in CDCl_3 (Table 4, entry 4).

¹H NMR (400 MHz, CDCl₃) δ 4.78 – 4.67 (m, 1H), 4.59 – 4.51 (m, 1H), 4.12 – 4.04 (m, 1H), 1.88 – 1.65 (m, 2H), 1.41 – 1.29 (m, 4H), 0.94 – 0.89 (m, 3H).

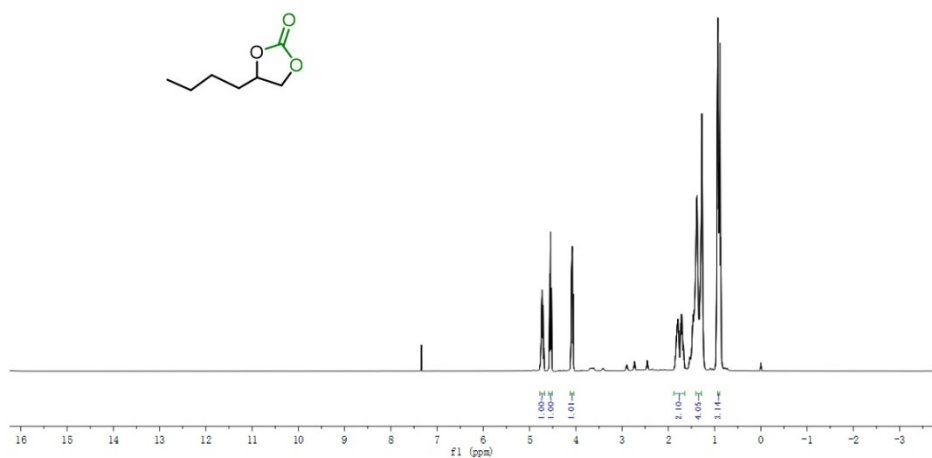


Fig. S6. Crude ¹H NMR spectrum of cyclic carbonate from 1,2-epoxyhexane in CDCl₃ (Table 4, entry 5).

¹H NMR (400 MHz, CDCl₃) δ 4.88 – 4.74 (m, 1H), 4.57 – 4.35 (m, 2H), 3.70 – 3.48 (m, 4H), 1.61 – 1.50 (m, 2H), 1.35 (d, 2H), 0.92 – 0.88 (m, 3H).

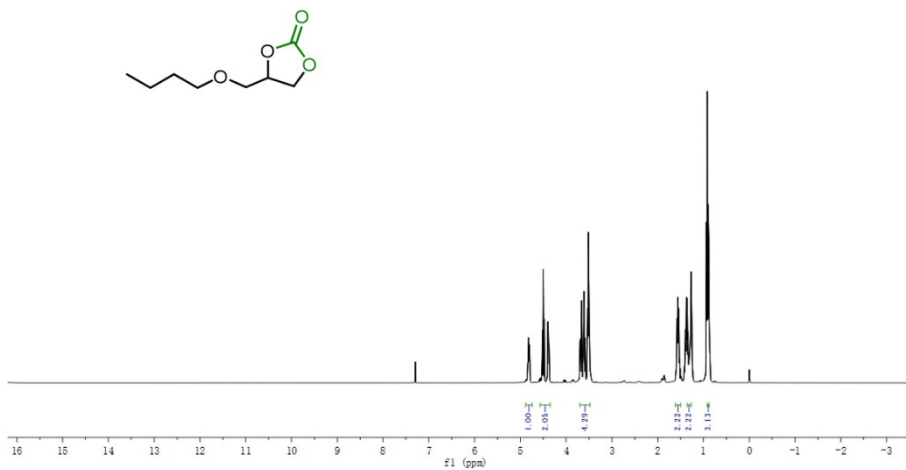


Fig. S7. Crude ¹H NMR spectrum of cyclic carbonate from butyl glycidyl ether in CDCl₃ (Table 4, entry 6).

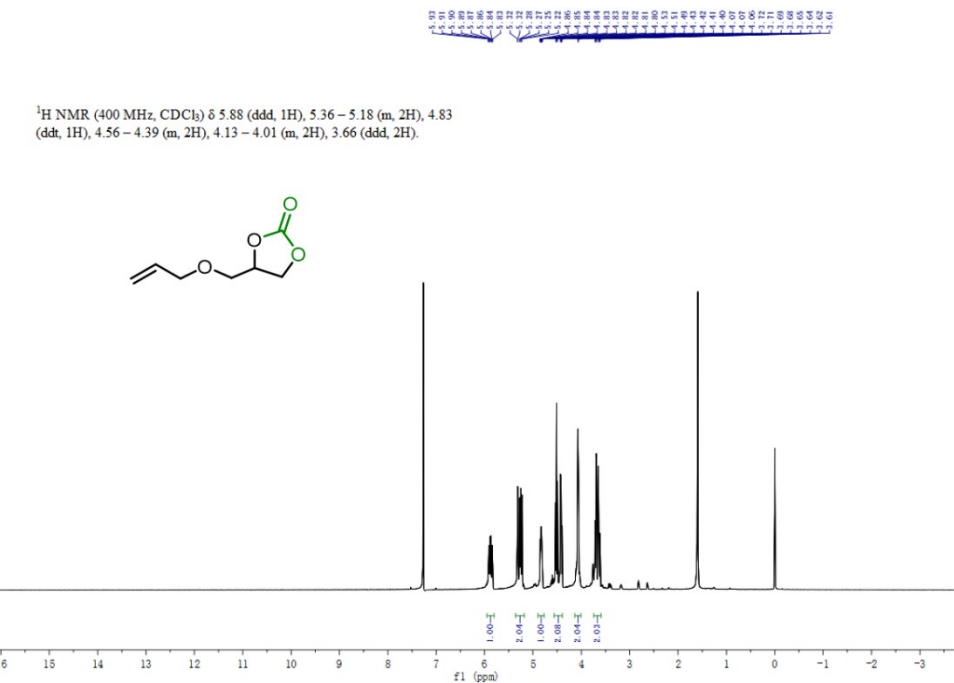


Fig. S8. Crude ^1H NMR spectrum of cyclic carbonate from allyl glycidyl ether in CDCl_3 (Table 4, entry 7).

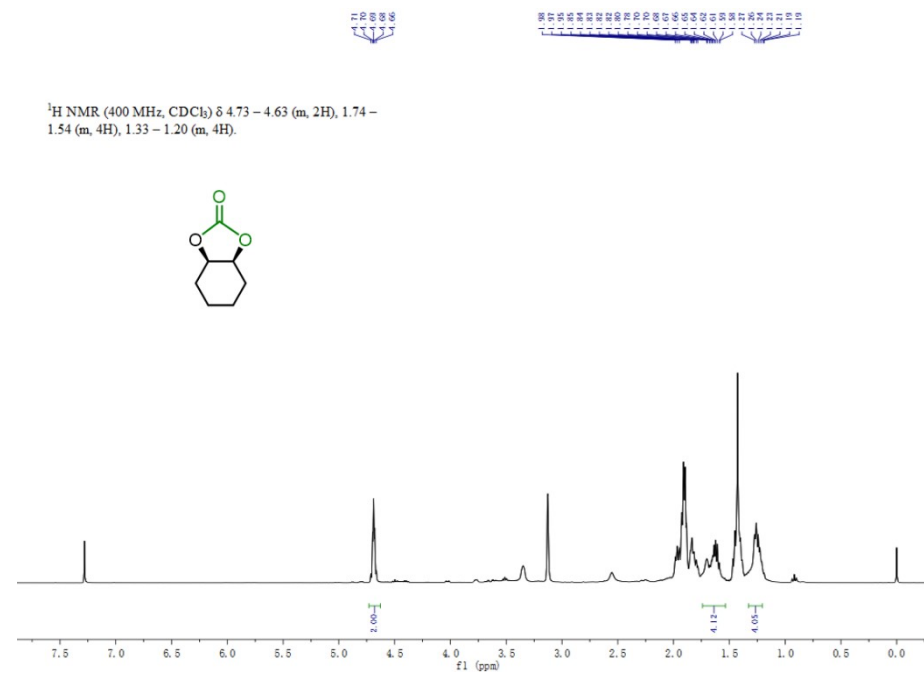


Fig. S9. Crude ^1H NMR spectrum of cyclic carbonate from cyclohexene oxide in CDCl_3 (Table 4, entry 8).

Comparisons of the catalytic activity of N₄-PIL-2.

Table S1. The heterogeneous catalysts for the cycloaddition reactions of epichlorohydrin and CO₂ at ambient pressure (0.1 MPa).

Catalyst	Catalyst Amount	Epoxide Amount	T (°C)	t (h)	P (MPa)	Con. (%) (TOF) ^a	Ref.
UIIP	0.150 mmol	38.4 mmol	110	21	0.1	98.0 (11.9)	S1
IP-1	0.300 mmol	10.0 mmol	100	18	0.1	76.0 (1.41)	S2
Ionization imidazole MOF	0.052 mmol	10.0 mmol	120	24	0.1	93.0 (7.45)	S3
CCTF-350	10.0 mg	10.0 mmol	120	24	0.1	95.0 (18.8)	S4
PEAMCl	100.0 mg	10.0 mmol	120	8	0.1	93.3 (10.7)	S5
DB10%- Pa-Tp	0.011 mmol	5.0 mmol	120	96	0.1	99.0 (4.40)	S6
PVIm-6-SCD	0.5 mol %	10.0 mmol	50	24	0.1	98.2 (1.40)	S7
CPP-IL	30.0 mg	12.7 mmol	100	24	0.1	99.0 (4.00)	S8
N₄-PIL-2	0.012 mmol	12.7 mmol	100	24	0.1	98.0 (42.4)	This work

^a parantheses are TOF (h⁻¹) values calculated with the help of reported data.

Table S2. The heterogeneous catalysts for the cycloaddition reactions of epichlorohydrin and CO₂.

Catalyst	Catalyst Amount	Epoxide Amount	T (°C)	t (h)	P (MPa)	Con. (%)	Ref.
P(DMAEMA-EtOH)Br	50 mg	14.3 mmol	110	3	2.0	90.4	S9
PIM2	0.2 mol %	10.0 mmol	130	4	1.0	92.0	S10
V-PCIF-Br	2.9 mol %	5.0 mmol	100	6	1.0	98.0	S11
ZnTPy-BIM4/CNTs-3	Substrate/Catalyst=1450		120	2.5	1.5	98.0	S12
MIL-101(Cr)-(Alm) ₂ ZnBr ₂	100 mg	35.7 mmol	120	1	1.0	99.4	S13
3-IPMP-EtI	0.5 mol %	30.0 mmol	90	5	1.0	90	S14
SBA16-PIL-Br	50.0 mg	5 mL	120	4	1.5	90.0	S15
PIL-4	20.0 mg	5.0 mmol	100	12	1.0	99.7	S16
HP-[BZPhIm]Cl-DCX-1	30.0 mg	5.0 mmol	120	5	1.0	99.9	S17
PHUs	[PHU urethane groups]/[epoxide] = 0.20		120	16	5.2	92.0	S18
PEAMCl	100.0 mg	10 mmol	120	2	1.0	98.7	S5
N₄-PIL-2	0.012 mmol	12.7 mmol	100	4	1.0	99.6	This work

Cartesian Coordinates (Å) of the Optimized Structures.

Table S3. Cartesian Coordinates (Å) of the Optimized Structures.

Optimized Structures A

	x	y	z
N	-13.057202	-1.461949	-0.416622
C	-11.686635	-3.618786	0.188701
C	-9.198194	-3.081937	-0.218757
N	-9.051486	-0.612187	-1.052841
C	-11.403086	0.341911	-1.160603
C	-15.711631	-1.096954	-0.294087
C	-17.36152	-2.828852	0.492939
C	-6.750708	0.774275	-1.810972
C	-4.511218	0.387701	-0.032802
C	-2.542894	2.45409	-0.517306
N	-0.19335	2.034275	0.849162
C	1.414514	4.296798	0.719267
C	3.882209	4.037894	2.183051
N	5.861368	2.753066	0.77685
C	8.362429	3.082001	1.880045
C	10.449075	1.939376	0.265153
N	10.464217	-0.823013	0.385918
C	12.521627	-1.939148	-1.095329
C	12.530725	-4.821367	-0.84917
N	10.255129	-6.096997	-1.752778
H	-12.578155	-5.331613	0.847635
H	-7.53603	-4.242964	0.0253
H	-11.900901	2.235461	-1.740357
H	-16.279606	0.776101	-0.911372
H	-16.830889	-4.708247	1.126754
H	-19.359104	-2.361059	0.520094
H	-7.285887	2.775296	-1.861309
H	-6.267835	0.200346	-3.744613
H	-3.635947	-1.472248	-0.328336
H	-5.153935	0.477881	1.941775
H	-3.420081	4.309809	-0.053493
H	-2.093265	2.523969	-2.549548
H	-0.593308	1.698775	2.71133
H	0.38994	5.985785	1.420316
H	1.880156	4.647863	-1.274299
H	3.493479	3.18431	4.066632
H	4.573089	5.958367	2.575395
H	5.472074	0.881036	0.53009
H	8.513128	2.317746	3.832653
H	8.706575	5.125739	2.03975
H	12.281612	2.761216	0.865729
H	10.149294	2.501121	-1.713199

H	10.695398	-1.349062	2.233599
H	14.39591	-1.183138	-0.533415
H	12.233852	-1.407809	-3.08752
H	12.810777	-5.317474	1.155794
H	14.174668	-5.584504	-1.858038
H	10.173577	-5.995897	-3.677275
H	8.718044	-5.127005	-1.099893

Optimized Structures B

	x	y	z
N	-7.224333	4.473169	1.746283
C	-6.001194	2.587608	0.385731
C	-3.970545	3.675414	-0.76613
N	-3.953079	6.203324	-0.117945
C	-5.93144	6.658383	1.413634
C	-9.455206	4.24577	3.218247
C	-10.920701	2.197026	3.277716
C	-2.024806	8.066139	-0.875842
C	0.244377	8.139001	0.907162
C	2.236175	9.993393	-0.061428
N	4.504375	9.981441	1.506107
C	6.36285	11.843182	0.584911
C	8.792965	11.888575	2.140132
N	10.682539	10.11054	1.245688
C	13.124706	10.385389	2.478084
C	15.100533	8.583658	1.415456
N	14.571272	5.976657	2.146558
C	16.276179	4.087426	1.07112
C	15.319708	1.421688	1.680652
N	12.818339	0.834116	0.649602
H	-6.665254	0.659626	0.35933
H	-2.545096	2.866069	-1.987115
H	-6.439913	8.468013	2.211006
H	-9.860987	5.937065	4.30768
H	-10.561456	0.50211	2.175412
H	-12.581874	2.195822	4.4816
H	-2.960529	9.909807	-0.987528
H	-1.441131	7.55815	-2.796303
H	1.081213	6.246467	1.065249
H	-0.388256	8.686149	2.810699
H	1.377763	11.903543	-0.236555
H	2.80758	9.440837	-1.98293
H	4.017983	10.482097	3.310051

H	5.537283	13.7654	0.545918
H	6.857864	11.347905	-1.368282
H	8.311656	11.648095	4.176653
H	9.619906	13.789394	1.989045
H	10.058292	8.281084	1.304179
H	13.023655	10.125845	4.564178
H	13.777052	12.337637	2.180039
H	16.995183	9.225929	2.03203
H	15.060839	8.692694	-0.657809
H	14.604303	5.836408	4.073948
H	18.251502	4.302602	1.740736
H	16.304337	4.359537	-0.989941
H	15.250975	1.204923	3.751646
H	16.692134	0.022437	1.006711
H	12.957498	0.517969	-1.250489
H	11.712486	2.414744	0.837153
C	6.956207	3.992422	3.647062
C	6.031588	3.093179	1.185341
O	8.301745	4.58108	1.35399
C	6.335164	0.393093	0.40184
Cl	6.301367	0.131785	-3.009015
H	7.925624	2.677912	4.908648
H	6.019923	5.608196	4.52311
H	4.46499	4.110791	0.30495
H	4.766119	-0.765655	1.09779
H	8.147962	-0.371748	1.052925

Optimized Structures C

	x	y	z
N	-12.098996	-1.904091	0.101906
C	-10.584053	-4.023003	-0.229774
C	-8.302668	-3.200834	-1.099637
N	-8.429725	-0.60082	-1.306594
C	-10.736224	0.154842	-0.563148
C	-14.637417	-1.815036	0.969267
C	-16.048564	-3.84387	1.452551
C	-6.373815	1.084262	-2.146705
C	-4.076208	0.967007	-0.407223
C	-2.112785	2.950188	-1.150944
N	0.125229	2.817936	0.457348
C	1.803504	4.996782	0.020615
C	4.154754	4.92744	1.682683
N	6.150102	3.369749	0.627953

C	8.436462	3.346015	2.1571
C	10.544071	1.85916	0.887238
N	9.890033	-0.813514	0.644752
C	11.811734	-2.304953	-0.670711
C	10.896796	-5.021351	-1.067019
N	8.593506	-5.268091	-2.575632
H	-11.233772	-5.90866	0.201361
H	-6.610928	-4.244448	-1.571108
H	-11.409199	2.082103	-0.527817
H	-15.329694	0.104008	1.203647
H	-15.399812	-5.776769	1.205914
H	-17.969094	-3.589304	2.128104
H	-7.167818	2.995502	-2.207278
H	-5.881076	0.548434	-4.088039
H	-3.213826	-0.917489	-0.462517
H	-4.689795	1.288409	1.553806
H	-3.011584	4.848861	-1.104159
H	-1.509218	2.645705	-3.119907
H	-0.447133	2.891155	2.30342
H	0.787255	6.799792	0.332469
H	2.404876	4.969647	-1.9672
H	3.598757	4.369261	3.636157
H	4.893684	6.863952	1.842648
H	5.556314	1.557397	0.336121
H	8.114116	2.581558	4.090046
H	9.070331	5.310557	2.409829
H	12.323382	2.159462	1.950092
H	10.835369	2.617871	-1.024667
H	9.614362	-1.560454	2.406897
H	13.651748	-2.313983	0.335953
H	12.144955	-1.410132	-2.519985
H	10.560136	-5.892782	0.795652
H	12.408229	-6.130661	-1.955048
H	8.988912	-4.853452	-4.418501
H	7.3602	-3.903097	-1.982473
C	1.492552	-2.4551	3.029985
O	-0.694953	-2.853063	3.120122
O	3.678694	-2.099575	2.979467

References

S1. M. A. Ziaeef, Y. Tang, H. Zhong, D. Tian and R. Wang, *ACS Sustainable Chemistry & Engineering*, 2018, **7**,

2380-2387.

- S2. Y. Zhang, E.-S. M. El-Sayed, K. Su, D. Yuan and Z. Han, *Journal of CO₂ Utilization*, 2020, **42**, 101301.
- S3. J. Liang, R. P. Chen, X. Y. Wang, T. T. Liu, X. S. Wang, Y. B. Huang and R. Cao, *Chem Sci*, 2017, **8**, 1570-1575.
- S4. T. T. Liu, R. Xu, J. D. Yi, J. Liang, X. S. Wang, P. C. Shi, Y. B. Huang and R. Cao, *ChemCatChem*, 2018, **10**, 2036-2040.
- S5. X. Wang, Q. Dong, Z. Xu, Y. Wu, D. Gao, Y. Xu, C. Ye, Y. Wen, A. Liu, Z. Long and G. Chen, *Chemical Engineering Journal*, 2021, **403**, 126460.
- S6. J. Cao, W. Shan, Q. Wang, X. Ling, G. Li, Y. Lyu, Y. Zhou and J. Wang, *ACS Appl Mater Interfaces*, 2019, **11**, 6031-6041.
- S7. Y. Xie, J. Liang, Y. Fu, M. Huang, X. Xu, H. Wang, S. Tu and J. Li, *Journal of Materials Chemistry A*, 2018, **6**, 6660-6666.
- S8. C. Cui, R. Sa, Z. Hong, H. Zhong and R. Wang, *ChemSusChem*, 2020, **13**, 180-187.
- S9. T. Ying, X. Tan, Q. Su, W. Cheng, L. Dong and S. Zhang, *Green Chemistry*, 2019, **21**, 2352-2361.
- S10. Y. Wang, J. Nie, C. Lu, F. Wang, C. Ma, Z. Chen and G. Yang, *Microporous and Mesoporous Materials*, 2020, **292**, 109751.
- S11. G. Chen, X. Huang, Y. Zhang, M. Sun, J. Shen, R. Huang, M. Tong, Z. Long and X. Wang, *Chemical Communications*, 2018, **54**, 12174-12177.
- S12. S. Jayakumar, H. Li, J. Chen and Q. Yang, *ACS Appl Mater Interfaces*, 2018, **10**, 2546-2555.
- S13. M. Zou, W. Dai, P. Mao, B. Li, J. Mao, S. Zhang, L. Yang, S. Luo, X. Luo and J. Zou, *Microporous and Mesoporous Materials*, 2021, **312**, 110750.
- S14. W. Zhang, Y. Mei, P. Wu, H.-H. Wu and M.-Y. He, *Catalysis Science & Technology*, 2019, **9**, 1030-1038.
- S15. R. Qu, Z. Ren, N. Li, F. Zhang, Z. J. Zhang and H. Zhang, *Journal of CO₂ Utilization*, 2020, **38**, 168-176.
- S16. H. Song, Y. Wang, M. Xiao, L. Liu, Y. Liu, X. Liu and H. Gai, *ACS Sustainable Chemistry & Engineering*, 2019, **7**, 9489-9497.
- S17. H. Song, Y. Wang, Y. Liu, L. Chen, B. Feng, X. Jin, Y. Zhou, T. Huang, M. Xiao, F. Huang and H. Gai, *ACS Sustainable Chemistry & Engineering*, 2021, **9**, 2115-2128.
- S18. S. Motokucho and H. Morikawa, *Chemical Communications*, 2020, **56**, 10678-10681.